EVALUATION OF BREAST CANCER PROLIFERATION IN A THREE-DIMENSIONAL IMAGE USING SKELETONIZATION TECHNIQUE

N. Subashini
Post Doctoral Research Scholar
Department of Mathematics
Sathyabama Instt. of Science & Tech.
Chennai, Tamilnadu
subashini.sams@gmail.com

K. Thiagarajan
Professor
Department of Mathematics
Rajalakshmi Instt. of Technology
Chennai, Tamilnadu
vidhyamannan@yahoo.com

E. G. Rajan
Promoter Director
Pentagram Research UK Ltd.
Birmingham, West Midlands
England, United Kingdom
dr.rajaneg@gmail.com

Abstract

Based on the experimental evidence available so far, most of the breast cancer proliferation evaluation methods are not reliable enough to make firm conclusions about their clinical value and use. Unfortunately, none of such recent technologies for cancer proliferation has been tried as a conventional 3D mammography technique. After confirming presence of cancer in a woman's breast, it is important to find out in which direction(s) the cancer is likely to spread. It is in this context, a novel technique to evaluate cancer proliferation using a 3D image skeletonization method is proposed.

Keywords: Breast Cancer, Lactal Carcinoma, 3D Breast Cancer Spread

1. Introduction

Given a **three dimensional mammography image**, one can detect the directions of cancer proliferation using a novel 3D skeletonization algorithm. 3D skeletonization is basically a surface removal operation of thinning with some additional constraint that the corner voxels are preserved while removing the surfaces.

Thinning and Skeletonization of 3D Images

After confirming presence of cancer in a woman's breast, it is important to predict in which direction(s) the cancer is likely to spread. It is in this context, a novel technique to evaluate cancer proliferation using 3D image skeletonization method is proposed. Thinning a 3D image is the reverse process of 3D contouring. Given a 3D solid object like an onion, one peels it off to the extent it is required. Continuous peeling of a 3D object results in the final 3D object, which cannot be further peeled. Fig. 1 shows the peeling off process of a hypothetical 3D cube like object with a boundary, till a 3D object without boundary is obtained.

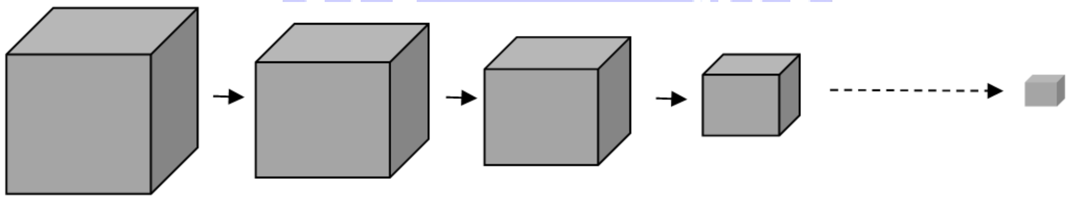

Fig. 1: Thinning process of a cube like solid object

Thinning process could be well understood with the help of a 3D array of size 5×5×5 shown in Fig. 2 and the result of step wise thinning it.

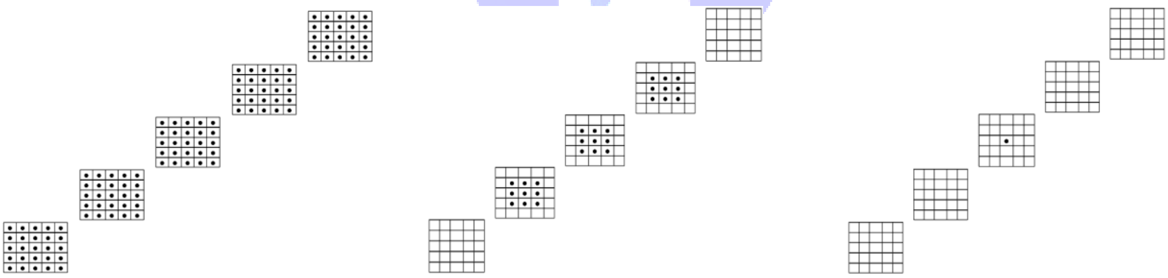

Input 3D array of size 5×5×5 | 3D array of size 5×5×5 thinned once | 3D array of size 5×5×5 thinned twice

Fig. 2: 3D array of size 5×5×5 and the result of step wise thinning it

3D skeletonization of an image is essentially a 3D thinning process with the exception that skeletonization retains all corner voxels. Fig. 3 shows a 3D array of size 5×5×5 and the result of step wise skeletonizing it.

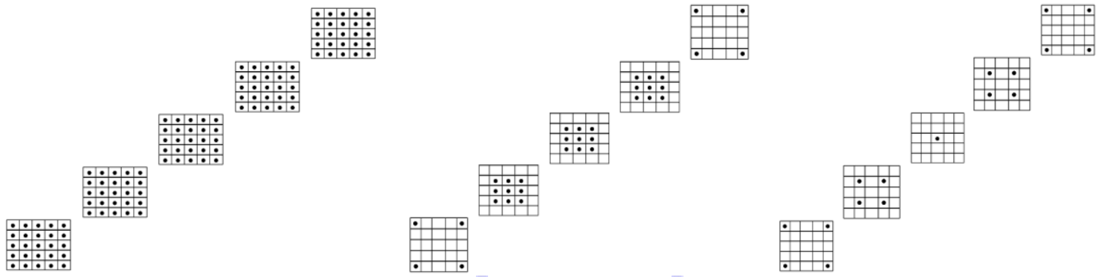

Input 3D array of size 5×5×5 | 3D array of size 5×5×5 skeletonized once | 3D array of size 5×5×5 skeletonized twice

Fig. 3: 3D array of size 5×5×5 and the result of step wise skeletonizing it

Fig. 4 shows a 3D solid cube of size 100×100×100 and its skeletonized version. It also shows a 3D image called "Cell Fract" and its skeletonized version.

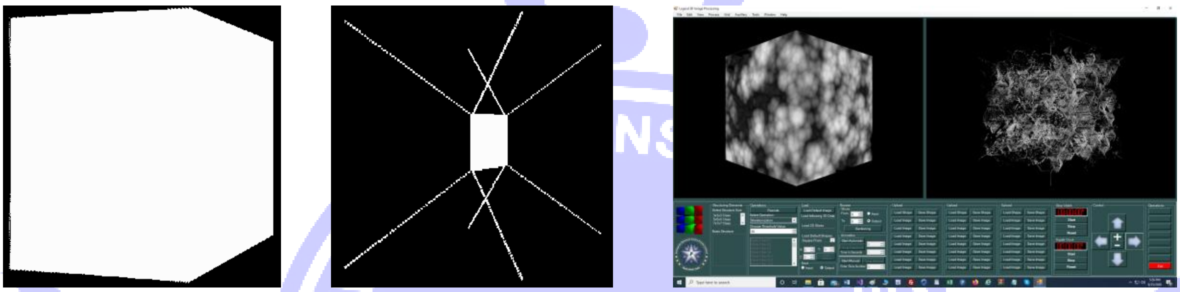

3D solid cube of size 100×100×100 | Skeleton of the cube | 3D image called "Cell Fract" of size 256×256×256 and its skeletonized version

Fig. 4: Skeletonization of 3D images

Courtesy: Pentagram Technologies, Hyderabad, India

Procedure to thin a 3D digital image

Given a 3D digital image, scan it with a 3×3×3 empty window, voxel wise. At each position do the following. Read the 3D image voxels under the 3D scanning window. Find out the largest voxel value (R,G,B) and the smallest value among the 27 values. Calculate the difference between the largest and the smallest voxel values. If the difference value is less than or equal to a user defined threshold value then ***remove all surface boundaries of the 3D sub image*** scanned by the 3D window and retain the central voxel value. If the difference value is greater than the threshold value then just move the 3D scanning window to the next position. Scan the entire 3D image and do the same as above. This yields the 3D image thinned by one 3D surface boundary. Repeat this thinning procedure until the output image does not show up any 3D surface boundary. Finally, one arrives at the completely thinned image with all surface boundaries removed.

Procedure to skeletonize a 3D digital image

Given a 3D digital image, scan it with a 3×3×3 empty window, voxel wise. At each position do the following. Read the 3D image voxels under the 3D scanning window. Find out the largest voxel value (R,G,B) and the smallest value among the 27 values. Calculate the difference between the largest and the smallest voxel values. If the difference value is less than or equal to a user defined threshold value then ***remove all surface boundaries other than corner pixels of the 3D sub image*** scanned by the 3D window and retain the central voxel value. If the difference value is greater than the threshold value then just move the 3D scanning window to the next position. Scan the entire 3D image and do the same as above. This yields the 3D image skeletonized by one 3D surface boundary. Repeat this skeletonization procedure until the output 3D image does not show up any 3D boundary. Finally, one arrives at the completely skeletonized 3D image with all boundaries removed other than 3D corners.

2. Skeletonization of 3D Images

Getting 3D raw data of breast cancer images has been found to be a challenging task while carrying out this research, the reason being 'confidentiality' involved in dealing with patients' medical data. Hence a hypothetical 3D model, which is a diagrammatic representation of surface outline of a female breast and breast cancer, is considered here, as an alternative, in order to test the algorithms given in this paper. This 3D gray image of size 462×549×121 consists of two values '0' and '255' for the Red, Green and Blue components. Two kinds of approaches to process 3D images are described in this paper: (i) processing of 3D images using 2D algorithms (this method is called 2.5D processing of 3D images) and (ii) processing of 3D images using 3D algorithms (this method is called 3D processing of 3D images). 3D skeletonization of 3D images is what is discussed here to detect directions of cancer proliferation.

Approach # 1: 2.5D processing of 3D images

In this case, given 3D image is processed slice wise. For example, each slice of given 3D image is thinned or skeletonized using 2D thinning and 2D skeletonization algorithms respectively. After processing the 3D image slice wise, the processed slices are assembled to form the processed 3D image. Fig. 5 shows 121 slices of a hypothetical 3D model of breast cancer. This gives an apparent look of a hollow female breast with an imaginary breast cancer in the form of a three dimensional star.

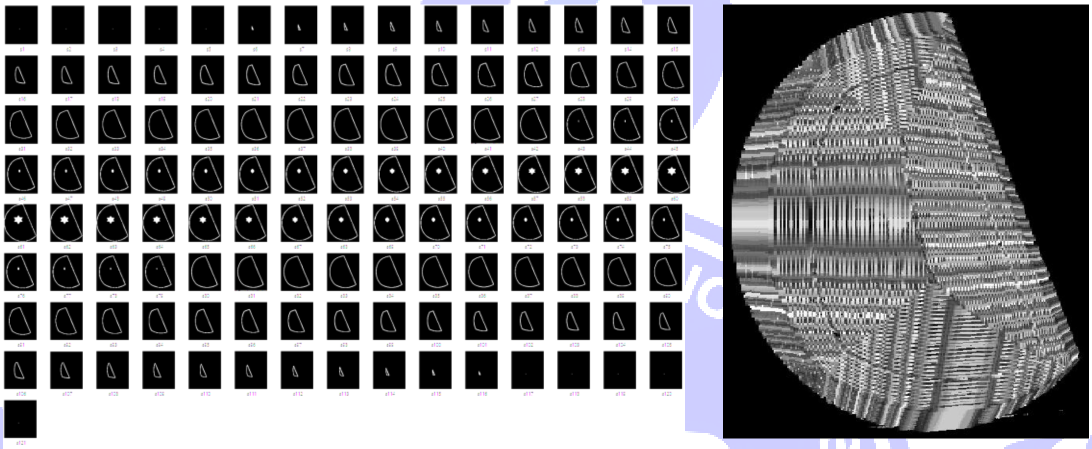

121 slices of a hypothetical 3D model of breast cancer Hypothetical 3D model

Fig. 5: 121 slices of a hypothetical 3D model of breast cancer

Fig. 6 shows the sectioned slices from 43 to 79 from the image shown in Fig. 5.

Slices from 43 to 79 of image shown in Fig. 6 3D model

Fig. 6: Hypothetical 3D model of breast cancer and its sectioned view

Fig. 7 shows 121 slices of 2.5D skeletonized hypothetical 3D model of breast cancer. The 3D model created using all the 121 slices shown in Fig. 7 will not display the skeletonized version of the breast cancer. Hence, the slices from 43 to 79, are considered here to create a 3D model. Fig. 8 shows the 2.5D skeleton model of slices from 43 to 79 of the hypothetical 3D model of breast cancer.

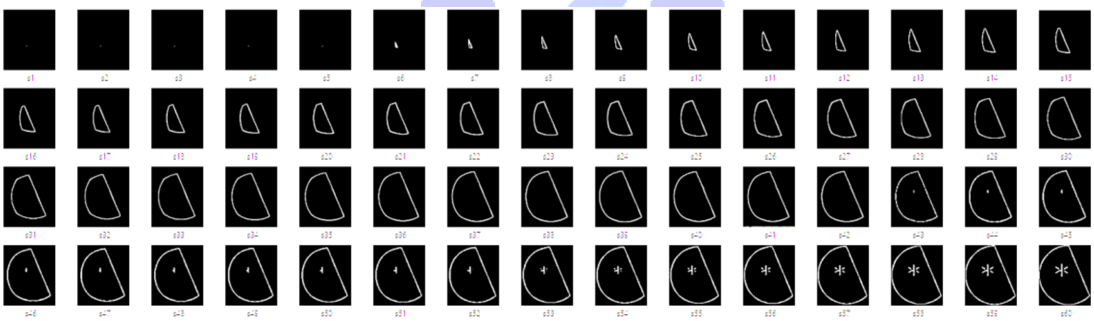

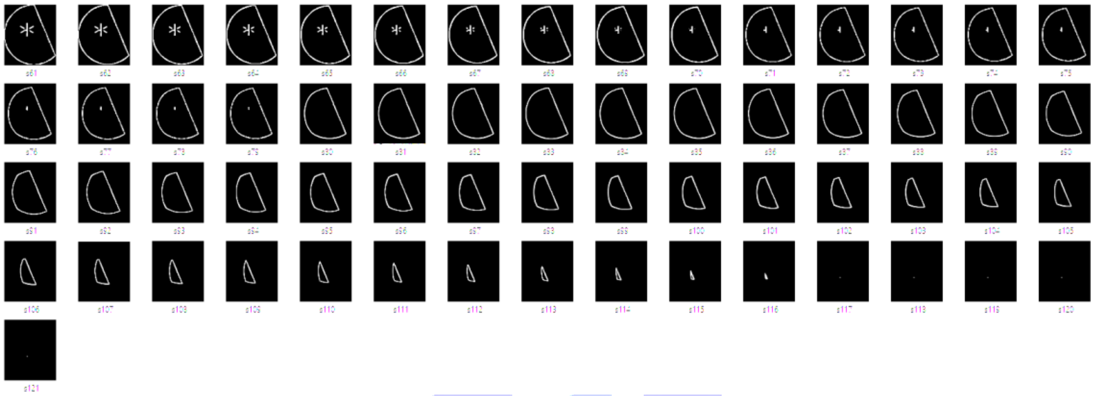

Fig. 7: Skeleton slices of a hypothetical 3D model of breast cancer

Fig. 8 shows the 2.5D skeleton model of slices from 43 to 79 of the hypothetical 3D model of breast cancer as well as its 3D skeletonized version. One can clearly see the difference between the 2.5D skeletonized image and 3D skeletonized image from Fig. 8.

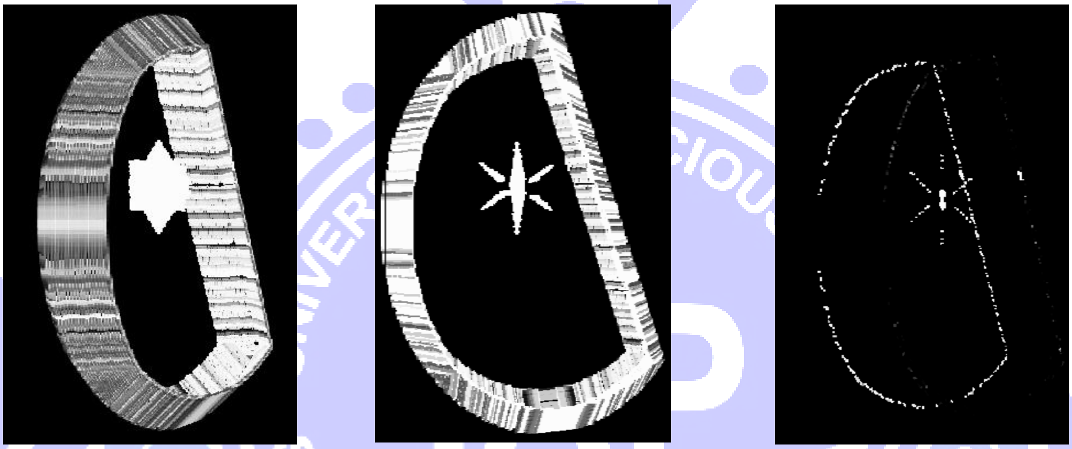

Hypothetical 3D model of breast Cancer with slices from 43 to 79 | 2.5D skeleton of the 3D model of breast cancer with slices from 43 to 79 | 3D skeleton of the 3D model of breast cancer with slices from 43 to 79

Fig. 8: 2.5D and 3D skeleton models of slices of 43 to 79 of hypothetical 3D model of breast cancer

3. Directions of Cancer Proliferation in a 3D Neighborhood of Size 3×3×3

In a three dimensional digital image, one can have 26 directions from a common point. In order to have a better understanding, let us consider a 3D neighborhood of size 3×3×3 shown in Fig. 9. This 3D neighborhood of size 3×3×3 is also visualized as a stack of three layers representing front plane, middle plane and rear plane of the structure shown in Fig. 9.

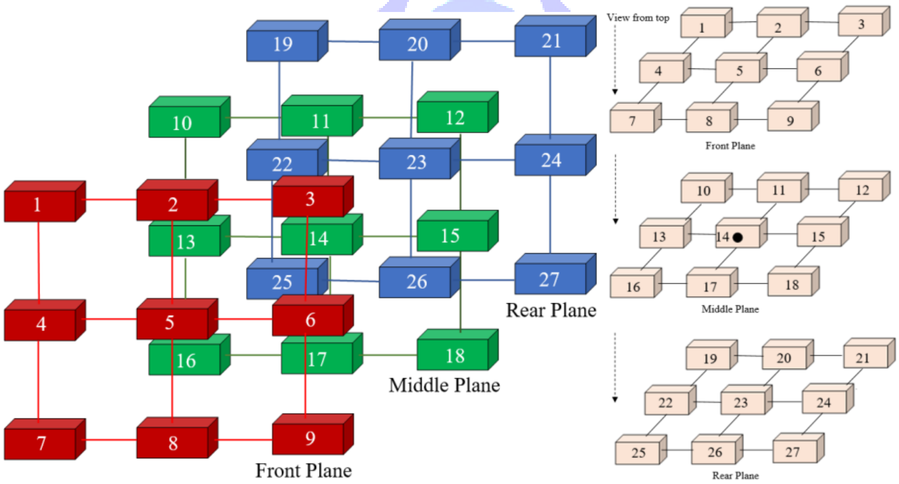

Fig. 9: 3D neighborhood structure of size 3×3×3 with labelled vertices

There are 26 directions of proliferation from the central cell (14th cell) where cancer seed is detected. They are presented below in Table 1. Table 2 presents total number of combinations of 67,108,864 directions called 3D scatter patterns.

Table 1: Directions from the central cell 14 to all other 26 vertices

$14 \rightarrow 1$	$14 \rightarrow 2$	$14 \rightarrow 3$	$14 \rightarrow 4$	$14 \rightarrow 5$	$14 \rightarrow 6$	$14 \rightarrow 7$
$14 \rightarrow 8$	$14 \rightarrow 9$	$14 \rightarrow 10$	$14 \rightarrow 11$	$14 \rightarrow 12$	$14 \rightarrow 13$	$14 \rightarrow 15$
$14 \rightarrow 16$	$14 \rightarrow 17$	$14 \rightarrow 18$	$14 \rightarrow 19$	$14 \rightarrow 20$	$14 \rightarrow 21$	$14 \rightarrow 22$
$14 \rightarrow 23$	$14 \rightarrow 24$	$14 \rightarrow 25$	$14 \rightarrow 26$	$14 \rightarrow 27$		

Table 2: Total of 67,108,864 three dimensional scatter patterns

${}^{26}C_0 = 1$	${}^{26}C_8 = 1562275$	${}^{26}C_{16} = 5311735$	${}^{26}C_{24} = 325$
${}^{26}C_1 = 26$	${}^{26}C_9 = 3124550$	${}^{26}C_{17} = 3124550$	${}^{26}C_{25} = 26$
${}^{26}C_2 = 325$	${}^{26}C_{10} = 5311735$	${}^{26}C_{18} = 1562275$	${}^{26}C_{26} = 1$
${}^{26}C_3 = 2600$	${}^{26}C_{11} = 7726160$	${}^{26}C_{19} = 657800$	
${}^{26}C_4 = 14950$	${}^{26}C_{12} = 9657700$	${}^{26}C_{20} = 230230$	
${}^{26}C_5 = 65780$	${}^{26}C_{13} = 10400600$	${}^{26}C_{21} = 65780$	
${}^{26}C_6 = 230230$	${}^{26}C_{14} = 9657700$	${}^{26}C_{22} = 14950$	
${}^{26}C_7 = 657800$	${}^{26}C_{15} = 7726160$	${}^{26}C_{23} = 2600$	

Fig. 10 shows some of the scatter patterns.

$$\text{Total number of directions in a } 3\times3\times3 \text{ rectangular lattice} = \sum_{i=0}^{26} {}^{26}C_i = 67,108,864$$

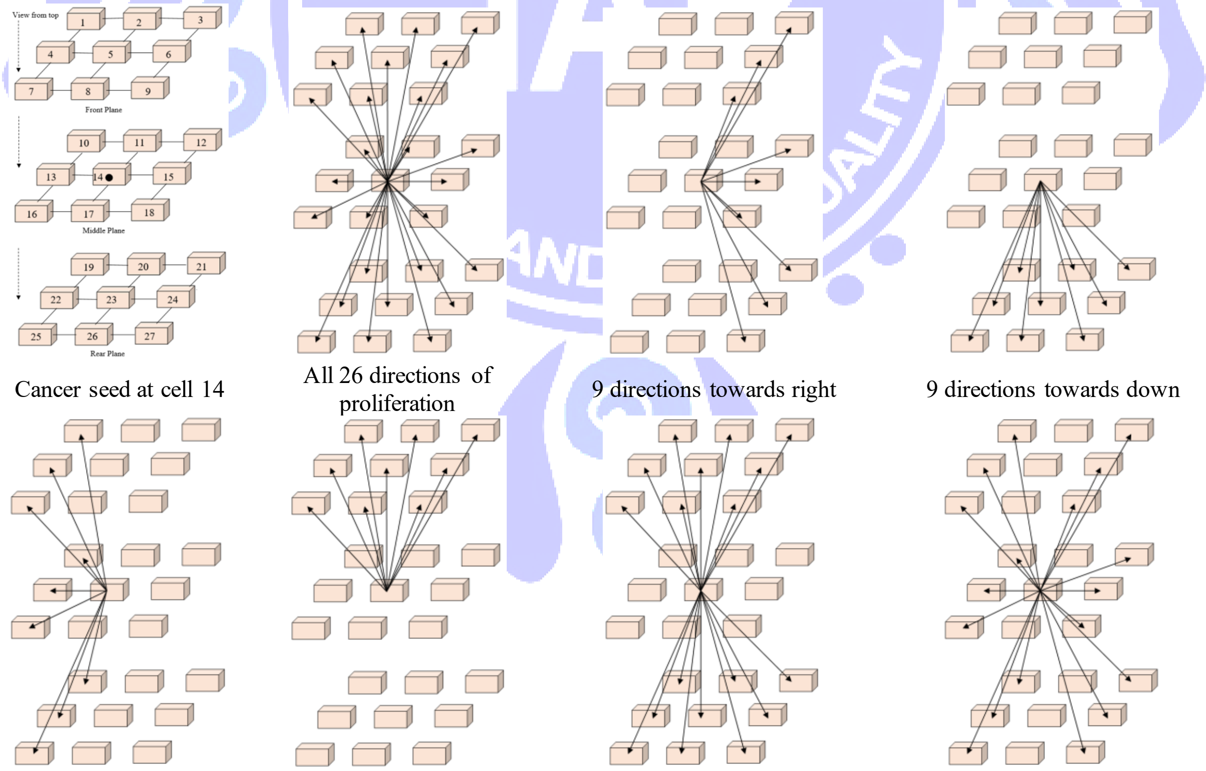

Cancer seed at cell 14 | All 26 directions of proliferation | 9 directions towards right | 9 directions towards down

9 directions towards left | 9 directions towards up | 9 directions towards up and 9 towards down | 9 directions towards left and 9 towards right

Fig. 10: Central cell 14 where cancer seed is detected, 26 possible directions of its proliferation, Cancer proliferation in 9 directions towards right and 9 towards down, Cancer proliferation in 9 directions towards left and 9 towards up, Cancer proliferation in 9 directions towards right and 9 towards down

Fig. 11 shows the distribution of number of 3D scatter patterns.

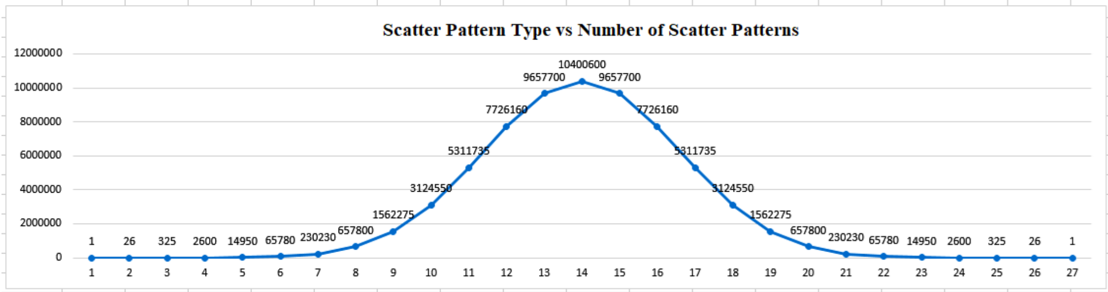

Fig. 11: Scatter pattern types (27) vs number of 3D scatter patterns

4. Formal Language Representation of 3D Scatter Patterns

Instead of representing number of 3D scatter patterns as a set for every scatter pattern type, a novel method of representing a set of 3D scatter patterns for a specific type as a string consisting of symbols from an alphabet A.

A = {<, >, 1,2,3,4,…,13,15,…, 27, →, *}

where <, >, * are delimiter symbols, 1,2,3,4,…,13,15,…,27 are vertex labels in the 3×3×3 neighborhood shown in Fig. 9. It is to be noted that the label 14 refers to the central cell where the cancer seed is detected and from where the cancer may proliferate to 26 different vertices. In what follows, a few of the 67,108,864 scatter patterns are presented as strings from the alphabet A.

Some of the scatter pattern strings

Node with degree 0: There is no scatter in this case.

Node with degree 1

There are 26 scatter patterns in this case.

<14→1>*<14→2>*<14→3>*<14→4>*<14→5>*<14→6>*<14→7>*<14→8>*<14→9>*<14→10>*<14→11>*<14→12>*<14→13>*<14→15>*<14→16>*<14→17>*<14→18>*<14→19>*<14→20>*<14→21>*<14→22>*<14→23>*<14→24>*<14→25>*<14→26>*<14→27>

Node with degree 2

There are 235 scatter patterns in this case.

<14→1>,<14→2>*<14→1>,<14→3>*<14→1>,<14→4>*<14→1>,<14→5>*<14→1>,<14→6>*<14→1>,<14→7>*<14→1>,<14→8>*<14→1>,<14→9>*<14→1>,<14→10>*<14→1>,<14→11>*<14→1>,<14→12>*<14→1>,<14→13>*<14→1>,<14→15>*<14→1>,<14→16>*<14→1>,<14→17>*<14→1>,<14→18>*<14→1>,<14→19>*<14→1>,<14→20>*<14→1>,<14→21>*<14→1>,<14→22>*<14→1>,<14→23>*<14→1>,<14→24>*<14→1>,<14→25>*<14→1>,<14→26>*<14→1>,<14→27>*<14→2>,<14→3>*<14→2>,<14→4>*<14→2>,<14→5>*<14→2>,<14→6>*<14→2>,<14→7>*<14→2>,<14→8>*<14→2>,<14→9>*<14→2>,<14→10>*<14→2>,<14→11>*<14→2>,<14→12>*<14→2>,<14→13>*<14→2>,<14→15>*<14→2>,<14→16>*<14→2>,<14→17>*<14→2>,<14→18>*<14→2>,<14→19>*<14→2>,<14→20>*<14→2>,<14→21>*<14→2>,<14→22>*<14→2>,<14→23>*<14→2>,<14→24>*<14→2>,<14→25>*<14→2>,<14→26>*<14→2>,<14→27>*<14→3>,<14→4>*<14→3>,<14→5>*<14→3>,<14→6>*<14→3>,<14→7>*<14→3>,<14→8>*<14→3>,<14→9>*<14→3>,<14→10>*<14→3>,<14→11>*<14→3>,<14→12>*<14→3>,<14→13>*<14→3>,<14→15>*<14→3>,<14→16>*<14→3>,<14→17>*<14→3>,<14→18>*<14→3>,<14→19>*<14→3>,<14→20>*<14→3>,<14→21>*<14→3>,<14→22>*<14→3>,<14→23>*<14→3>,<14→24>*<14→3>,<14→25>*<14→3>,<14→26>*<14→3>,<14→27>*<14→4>,<14→5>*<14→4>,<14→6>*<14→4>,<14→7>*<14→4>,<14→8>*<14→4>,<14→9>*<14→4>,<14→10>*<14→4>,<14→11>*<14→4>,<14→12>*<14→4>,<14→13>*<14→4>,<14→15>*<14→4>,<14→16>*<14→4>,<14→17>*<14→4>,<14→18>*<14→4>,<14→19>*<14→4>,<14→20>*<14→4>,<14→21>*<14→4>,<14→22>*<14→4>,<14→23>*<14→4>,<14→24>*<14→4>,<14→25>*<14→4>,<14→26>*<14→4>,<14→27>*<14→5>,<14→6>*<14→5>,<14→7>*<14→5>,<14→8>*<14→5>,<14→9>*<14→5>,<14→10>*<14→5>,<14→11>*<14→5>,<14→12>*<14→5>,<14→13>*<14→5>,<14→15>*<14→5>,<14→16>*<14→5>,<14→17>*<14→5>,<14→18>*<14→5>,<14→19>*<14→5>,<14→20>*<14→5>,<14→21>*<14→5>,<14→22>*<14→5>,<14→23>*<14→5>,<14→24>*<14→5>,<14→25>*<14→5>,<14→26>*<14→5>,<14→27>*<14→6>,<14→7>*<14→6>,<14→8>*<14→6>,<14→9>*<14→6>,<14→10>*<14→6>,<14→11>*<14→6>,<14→12>*<14→6>,<14→13>*<14→6>,<14→15>*<14→6>,<14→16>*<14→6>,<14→17>*<14→6>,<14→18>*<14→6>,<14→19>*<14→6>,<14→20>*<14→6>,<1

4→21>*<14→6>,<14→22>*<14→6>,<14→23>*<14→6>,<14→24>*<14→6>,<14→25>*<14→6>,<14→26>*<14→6>,<14→27>*<14→7>,<14→8>*<14→7>,<14→9>*<14→7>,<14→10>*<14→7>,<14→11>*<14→7>,<14→12>*<14→7>,<14→13>*<14→7>,<14→15>*<14→7>,<14→16>*<14→7>,<14→17>*<14→7>,<14→18>*<14→7>,<14→19>*<14→7>,<14→20>*<14→7>,<14→21>*<14→7>,<14→22>*<14→7>,<14→23>*<14→7>,<14→24>*<14→7>,<14→25>*<14→7>,<14→26>*<14→7>,<14→27>*<14→8>,<14→9>*<14→8>,<14→10>*<14→8>,<14→11>*<14→8>,<14→12>*<14→8>,<14→13>*<14→8>,<14→15>*<14→8>,<14→16>*<14→8>,<14→17>*<14→8>,<14→18>*<14→8>,<14→19>*<14→8>,<14→20>*<14→8>,<14→21>*<14→8>,<14→22>*<14→8>,<14→23>*<14→8>,<14→24>*<14→8>,<14→25>*<14→8>,<14→26>*<14→8>,<14→27>*<14→9>,<14→10>*<14→9>,<14→11>*<14→9>,<14→12>*<14→9>,<14→13>*<14→9>,<14→15>*<14→9>,<14→16>*<14→9>,<14→17>*<14→9>,<14→18>*<14→9>,<14→19>*<14→9>,<14→20>*<14→9>,<14→21>*<14→9>,<14→22>*<14→9>,<14→23>*<14→9>,<14→24>*<14→9>,<14→25>*<14→9>,<14→26>*<14→9>,<14→27>*<14→10>,<14→11>*<14→10>,<14→12>*<14→10>,<14→13>*<14→10>,<14→15>*<14→10>,<14→16>*<14→10>,<14→17>*<14→10>,<14→18>*<14→10>,<14→19>*<14→10>,<14→20>*<14→10>,<14→21>*<14→10>,<14→22>*<14→10>,<14→23>*<14→10>,<14→24>*<14→10>,<14→25>*<14→10>,<14→26>*<14→10>,<14→27>*<14→11>,<14→12>*<14→11>,<14→13>*<14→11>,<14→15>*<14→11>,<14→16>*<14→11>,<14→17>*<14→11>,<14→18>*<14→11>,<14→19>*<14→11>,<14→20>*<14→11>,<14→21>*<14→11>,<14→22>*<14→11>,<14→23>*<14→11>,<14→24>*<14→11>,<14→25>*<14→11>,<14→26>*<14→11>,<14→27>*<14→12>,<14→13>*<14→12>,<14→15>*<14→12>,<14→16>*<14→12>,<14→17>*<14→12>,<14→18>*<14→12>,<14→19>*<14→12>,<14→20>*<14→12>,<14→21>*<14→12>,<14→22>*<14→12>,<14→23>*<14→12>,<14→24>*<14→12>,<14→25>*<14→12>,<14→26>*<14→12>,<14→27>*<14→13>,<14→15>*<14→13>,<14→16>*<14→13>,<14→17>*<14→13>,<14→18>*<14→13>,<14→19>*<14→13>,<14→20>*<14→13>,<14→21>*<14→13>,<14→22>*<14→13>,<14→23>*<14→13>,<14→24>*<14→13>,<14→25>*<14→13>,<14→26>*<14→13>,<14→27>*<14→15>,<14→16>*<14→15>,<14→17>*<14→15>,<14→18>*<14→15>,<14→19>*<14→15>,<14→20>*<14→15>,<14→21>*<14→15>,<14→22>*<14→15>,<14→23>*<14→15>,<14→24>*<14→15>,<14→25>*<14→15>,<14→26>*<14→15>,<14→27>*<14→16>,<14→17>*<14→16>,<14→18>*<14→16>,<14→19>*<14→16>,<14→20>*<14→16>,<14→21>*<14→16>,<14→22>*<14→16>,<14→23>*<14→16>,<14→24>*<14→16>,<14→25>*<14→16>,<14→26>*<14→16>,<14→27>*<14→17>,<14→18>*<14→17>,<14→19>*<14→17>,<14→20>*<14→17>,<14→21>*<14→17>,<14→22>*<14→17>,<14→23>*<14→17>,<14→24>*<14→17>,<14→25>*<14→17>,<14→26>*<14→17>,<14→27>*<14→18>,<14→19>*<14→18>,<14→20>*<14→18>,<14→21>*<14→18>,<14→22>*<14→18>,<14→23>*<14→18>,<14→24>*<14→18>,<14→25>*<14→18>,<14→26>*<14→18>,<14→27>*<14→19>,<14→20>*<14→19>,<14→21>*<14→19>,<14→22>*<14→19>,<14→23>*<14→19>,<14→24>*<14→19>,<14→25>*<14→19>,<14→26>*<14→19>,<14→27>*<14→20>,<14→21>*<14→20>,<14→22>*<14→20>,<14→23>*<14→20>,<14→24>*<14→20>,<14→25>*<14→20>,<14→26>*<14→20>,<14→27>*<14→21>,<14→22>*<14→21>,<14→23>*<14→21>,<14→24>*<14→21>,<14→25>*<14→21>,<14→26>*<14→21>,<14→27>*<14→22>,<14→23>*<14→22>,<14→24>*<14→22>,<14→25>*<14→22>,<14→26>*<14→22>,<14→27>*<14→23>,<14→24>*<14→23>,<14→25>*<14→23>,<14→26>*<14→23>,<14→27>*<14→24>,<14→25>*<14→24>,<14→26>*<14→24>,<14→27>*<14→25>,<14→26>*<14→25>,<14→27>*<14→26>,<14→27>

3D scatter patterns for node with degree 3 to degree 25 are not given here.

Node with degree 26

There is only one 3D scatter pattern in this case.

<14→1>,<14→2>,<14→3>,<14→4>,<14→5>,<14→6>,<14→7>,<14→8>,<14→9>,<14→10>,<14→11>,<14→12>,<14→13>,<14→15>,<14→16>,<14→17>,<14→18>,<14→19>,<14→20>,<14→21>,<14→22>,<14→23>,<14→24>,<14→25>,<14→26>,<14→27>

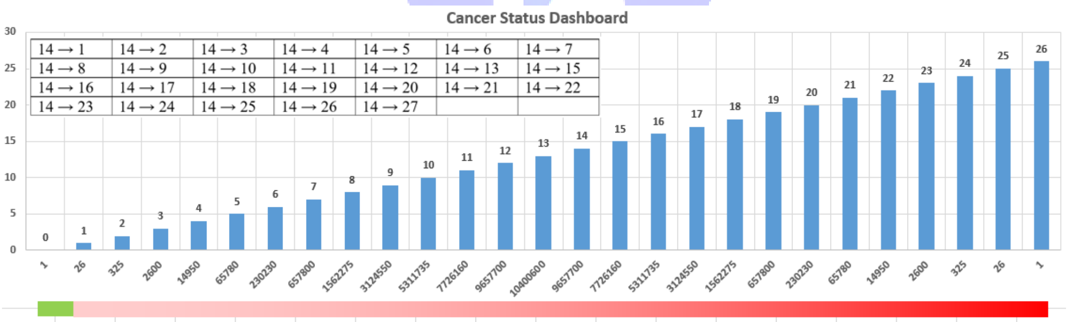

Fig. 12: Cancer status dashboard

5. Conclusions

Given a three dimensional scanned image of female breast, one can evaluate the present cancer proliferation status using the novel technique introduced in this paper. Skeletonization algorithm is used for detecting cancer proliferation in all 4Π steradians. With reference to Fig. 9, the degree of a node decides the status of cancer proliferation. The node with degree 26 could be seen to show that the cancer status has reached the final stage and this indicates the necessity to go in for surgery such as lumpectomy, quadrantectomy, partial mastectomy, or segmental mastectomy meaning removal only the part of the breast containing the cancer.

Acknowledgement

The authors thank all those who supported in this research, mainly scientists from Pentagram Research UK Ltd Birmingham, England and Pentagram Technologies, Hyderabad, India for providing ample opportunities to carry out this research.

References

1. A. J. Mendez, P. G. Tahoces, M. J. Lado, M. Souto, and J. J. Vidal, “Computer-aided diagnosis: Automatic detection of malignant masses in digitized mammograms,” Med Phys., vol. 25, pp. 957–64, Jun. 1998.
2. J. Tang, R. Rangayyan, J. Xu, I. E. Naqa, and Y. Yang, “Computer aided detection and diagnosis of breast cancer with mammography: Recent advances,” IEEE Trans. Inf. Technol. Biomed., vol. 13, no. 2, pp. 236–251, Mar. 2009.
3. M. Ladekarl, “Objective malignancy grading: A review emphasizing unbiased stereology applied to breast tumors,” APMIS Suppl., vol. 79, pp. 1–34, 1998.
4. T. M. Haygood, G. J. Whitman, E. N. Atkinson, R. G. Nikolova, S. Y. Sandoval, and P. J. Dempsey, “Results of a survey on digital screening mammography: Prevalence, efficiency, and use of ancillary diagnostic AIDS,” J. Amer. Coll. Radiol., vol. 5, pp. 585–92, Apr. 2008.
5. R. Schulz-Wendtland, K. P. Hermann, T.Wacker, and W. Bautz, “Current situation and future perspectives of digital mammography,” Radiologe, vol. 48, pp. 324–34, Apr. 2008.

About the Authors

Dr. N. Subashini is an active researcher in Mathematics. She Completed her Ph.D. from Mother Teresa Women’s University, Kodaikanal. She has published many research articles in various international and national journals and won best paper award. She has 20 years of teaching and research experience. Her area of interest includes various topics in Graph and Network Theory and Predictive Analytics.

Dr. K. Thiagarajan is a Professor of Mathematics at Rajalakshmi Institute of Technology Chennai. Under the affiliation of Anna University Chennai. He completed his Ph.D. from Mysore University and He completed his post-Doctoral research in Pentagram Research Centre Hyderabad. He has published over 120 research articles in various international and national journals. He has more than 20 years of teaching and research experience. His area of interest includes various topics in Graph and Networks like Coloring, Automata theory and DNA computing.

Prof. Dr. E. G. Rajan the Founder Chairman of Pentagram Group of Companies. He is an Electronics Engineer and a Professor of Signal Processing having about 50 years of experience in teaching, research and administration. He has a number of publications to his credit. His contribution to the state-of-the-art of Electronic Warfare and Support Measures has been well recognized in the Government and industrial sectors. He was a noted teacher in the department of Electrical Engineering of the Indian Institute of Technology, Kanpur. He received Distinguished Scientist and Man of the Millennium Award from Who is Who Bibliographical Records, Cambridge, 2000. He authored many books and research papers. He is the father of a novel paradigm Symbolic Computing in the Framework of Markov’s Constructive Mathematical Logic. His contribution to Computer Vision, Pattern Recognition, Modeling and Simulation, Artificial Intelligence and Machine Learning Could be seen in his research publications. Many of his PhD students were involved in the design of digital circuits using organic molecules. He has brought out a number of original patentable concepts. One such concept is Codon Space, which advocates the theory of Life Forms as Subspaces of the Information Space called Codon Space. Another concept is a Mathematical Transform, which goes by his name as Rajan Transform.